Available online at www.sciencedirect.com
SCIENCE DIRECT®
Computational Materials Science 36 (2006) 354–360
COMPUTATIONAL MATERIALS SCIENCE
www.elsevier.com/locate/commatsci

A fast and robust algorithm for Bader decomposition of charge density

Graeme Henkelman [a,*], Andri Arnaldsson [b], Hannes Jónsson [b,c]

[a] Department of Chemistry and Biochemistry, The University of Texas at Austin, Austin, TX 78712-0165, United States
[b] Department of Chemistry 351700, University of Washington, Seattle, WA 98195-1700, United States
[c] Faculty of Science, VR-II, University of Iceland, 107 Reykjavík, Iceland

Received 29 April 2004; received in revised form 1 December 2004; accepted 10 April 2005

Abstract

An algorithm is presented for carrying out decomposition of electronic charge density into atomic contributions. As suggested by Bader [R. Bader, Atoms in Molecules: A Quantum Theory, Oxford University Press, New York, 1990], space is divided up into atomic regions where the dividing surfaces are at a minimum in the charge density, i.e. the gradient of the charge density is zero along the surface normal. Instead of explicitly finding and representing the dividing surfaces, which is a challenging task, our algorithm assigns each point on a regular (x, y, z) grid to one of the regions by following a steepest ascent path on the grid. The computational work required to analyze a given charge density grid is approximately 50 arithmetic operations per grid point. The work scales linearly with the number of grid points and is essentially independent of the number of atoms in the system. The algorithm is robust and insensitive to the topology of molecular bonding. In addition to two test problems involving a water molecule and NaCl crystal, the algorithm has been used to estimate the electrical activity of a cluster of boron atoms in a silicon crystal. The highly stable three-atom boron cluster, B_3I is found to have a charge of -1.5 e, which suggests approximately 50% reduction in electrical activity as compared with three substitutional boron atoms.

PACS: 31.15.−p; 71.55.Cw; 72.80.cw; 61.72.Tt

Keywords: Atoms in molecules; Bader analysis; Electron density analysis; Atomic charges; Boron clusters; Linear scaling algorithm

1. Introduction

The properties of chemicals and materials are often described in terms of charge transfer between atoms and the presence of ionic charges or electric multipoles on atoms or molecules. Theoretical calculations producing estimates of the electronic charge distribution in the system can, in principle, provide this type of information but it is not clear how to extract it. Atomic charges in molecules or solids are not observables and, therefore, not defined by quantum mechanical theory. The output of quantum mechanical calculations is a continuous electronic charge density and it is not clear how one should partition electrons amongst fragments of the system such as atoms or molecules. Many different schemes have been proposed, some based on electronic orbitals and others based on only the charge density (see for example Ref. [1]).

The most commonly used orbital based method is the so-called Mulliken analysis. It can be applied when basis functions centered on atoms are used in the calculation of the electronic wavefunction of the system. The charge associated with the basis functions centered on a particular atom is then assigned to that atom. This can be a

* Corresponding author. Tel.: +1 512 471 4179.
E-mail address: henkelman@mail.utexas.edu (G. Henkelman).

0927-0256/$ - see front matter © 2005 Elsevier B.V. All rights reserved.
doi:10.1016/j.commatsci.2005.04.010

fast and useful way of determining partial charges on atoms but it has the major drawback that the analysis is sensitive to the choice of basis set. Furthermore, in the limit of an infinite basis, the assignment becomes arbitrary. As an extreme case, a complete basis set can be formed where all the basis functions are centered on just one atom in the system. The Mulliken analysis would then clearly be misleading as it would assign all the electrons in the system to that one atom. Moreover, many calculations are carried out with plane wave basis functions which are not associated with any particular atom in the system. Mulliken analysis is not applicable in such cases.

A different approach is to focus entirely on the charge density as has been proposed by Bader [2]. Space is then divided into regions by surfaces that run through minima in the charge density. More precisely, at a point on a dividing surface the gradient of the electron density has no component normal to the surface. We will refer to regions bounded by such dividing surfaces as *Bader regions*. Because this analysis is based solely on the charge density, it is rather insensitive to the basis set used in the electron wavefunction calculation and can be used to analyze plane wave based calculations as well as calculations using atomic basis functions. Furthermore, it can be used to analyze electronic density obtained by other means, for example from X-ray crystallography. Each Bader region often contains one nucleus, but this is not necessarily so, sometimes no nucleus is found within a Bader region. By integrating the electronic density within the Bader region where an atom's nucleus is located, and possibly adding the electronic charge in nearby regions that do not include a nucleus, the total charge on an atom can be estimated.

A common complaint about Bader analysis is the computational effort and complexity of the algorithms that have been developed [3,1]. Commonly used implementations [2,4,5] involve finding the critical points of the charge density where $\nabla\rho = 0$, followed by the construction of the zero-flux surfaces which intersect these points and then integration of the electronic density within each region. Several refinements have been made since the initial implementation of the method. Popelier improved the basin integration method by using Chebyshev polynomials [6], along with a bisection method [7] for finding dividing surfaces and increased integration accuracy around critical points [2]. Popelier has also suggested integrating the electric field on the dividing surface around atoms in order to find the enclosed charge through the divergence theorem [3]. Most recently Malcolm and Popelier [8,9] have used dynamic grid techniques introduced by Silvi and coworkers [10,11] in order to effectively treat complicated bonding topology. A very different approach was presented by Uberuaga et al. where multiple replicas of the system connected by springs form a discrete representation of an 'elastic sheet' that stretches along the dividing surface surrounding a given Bader region [12].

In this paper, a simple and fast method for carrying out Bader decomposition of electron density is presented. It is different from the methods mentioned above in that an explicit representation of the dividing surfaces is not used and no attempt is made to locate stationary points of the charge density. This makes the algorithm more robust. Algorithms that are commonly used today are known to have convergence problems in some cases (an example involving clusters of water molecules is given in Ref. [12]). As in several previous implementations of Bader analysis, such as TopMoD [10], InteGriTy [13], Extreme 94 [14], and MORPHY [4], it is assumed that the electron density is represented by its values on a regular grid in three-dimensions, but our method is different from previous methods in that only steepest ascent trajectories confined to the grid points are used to identify the Bader regions. The algorithm is robust since dividing surfaces and critical points do not need to be found explicitly. This makes the method applicable to systems with complicated bonding topology where the representation of the dividing surfaces is difficult. Although the dividing surfaces are not found explicitly, it is easy to render them for visualization after the analysis is complete. Bader regions which do not contain a nucleus [15] do not pose a problem because the method does not use the nuclear coordinates, neither in finding Bader regions nor in the integration of the electron density. Furthermore, no assumption about the shape of the Bader region is made in the integration of the electron density. Such an assumption is, for example, made when radial integration away from nuclei is used (see for example [13]). Such a procedure is valid when radial rays do not cross the dividing surface more than once but this is not always the case [16]. The number of arithmetic operations per grid point in our algorithm is insensitive to the size of the grid and the number of atoms in the system so the computational effort scales linearly with the number of grid points used in the representation of the electron density. A description of the algorithm will now be presented.

2. Grid based Bader decomposition

The input for the Bader decomposition is a charge density grid, that gives the value of the electron density specified on a regular grid of points in space. The spacing between the grid points should be fine enough that a linear interpolation between the points is a sufficiently good approximation in the bonding region between atoms. In order to find out which grid points belong to each of the Bader regions, a path of steepest ascent on the charge density grid is defined for each grid point. The set of grid points that have paths ending in the same

terminus of maximal charge density are members of the same Bader region. Typically (but not always, for example see Ref. [15]), these points of charge density maxima are located at atomic nuclei. The total electronic charge within a Bader region can then be approximated by the sum over the corresponding grid points.

Some caution is needed when analyzing charge density obtained by calculations based on pseudopotential representation of core electrons. An accurate representation of the density in the core region where the pseudowavefunction differs from the true wavefunction is not needed as long as there are no artificial minima in the charge density. Such minima can form, for example, close to the nucleus when using pseudopotentials for elements with few valence electrons. In some cases this problem can be alleviated by treating sub-valence electrons explicitly and representing fewer electrons with the pseudopotential. Otherwise, the value of the core electron density can be added to the value of the valence electron density at the grid points. It is easy to detect whether the Bader dividing surfaces that separate atomic regions lie inside core regions, and this option is included in our software.

The charge density grid points are assumed here to form an orthogonal lattice to simplify the description of the algorithm, but a generalization to a non-orthogonal lattice is straightforward. In order to associate each grid point with a Bader region, a path of steepest ascent in the charge density is found. To speed up the calculation, the paths are constrained to the grid points and a move from a given grid point can only be made to one of the 26 neighboring grid points. More specifically, a steepest ascent move from a grid point (i,j,k), is made along the direction which maximizes the charge density gradient, $\nabla\rho$, is calculated along the 26 possible directions, $\hat{r}$, towards adjacent grid points, using

$$\nabla\rho(i,j,k)\cdot\hat{r}(\mathrm{d}i,\mathrm{d}j,\mathrm{d}k)=\frac{\Delta\rho}{|\Delta\vec{r}|} \tag{1}$$

where $\mathrm{d}i$, $\mathrm{d}j$, $\mathrm{d}k$ are each assigned the values $\{-1,0,1\}$ but excluding $\mathrm{d}i=\mathrm{d}j=\mathrm{d}k=0$. The change in density

$$\Delta\rho=\rho(i+\mathrm{d}i,j+\mathrm{d}j,k+\mathrm{d}k)-\rho(i,j,k) \tag{2}$$

and the distance

$$|\Delta\vec{r}|=|\vec{r}(i+\mathrm{d}i,j+\mathrm{d}j,k+\mathrm{d}k)-\vec{r}(i,j,k)| \tag{3}$$

are evaluated between neighbors, where $\vec{r}(i,j,k)$ is the Cartesian vector to the grid point (i,j,k). The steepest ascent step selected, $\vec{r}(\mathrm{d}i,\mathrm{d}j,\mathrm{d}k)$, is the one that maximizes the positive values of $\nabla\rho(i,j,k)$. If there are no positive values, the point (i,j,k) is considered to be a charge density maximum.

Fig. 1 illustrates the algorithm. The starting point of the calculation is chosen to be (i_1,j_1,k_1). A steepest ascent path is followed until a charge density maximum m_1 is found. The number assigned to the maximum (1 in this case) is entered in an array for each point along the trajectory. In this way, each of the points along the path is assigned to Bader region 1. A steepest ascent path from each one of these points terminates at m_1. Then, the next point, (i_2,j_2,k_2), in the grid that has not already been assigned is taken as a starting point for a new steepest ascent path. The path is extended until it reaches a grid point that has already been assigned, or when a new maximum is found. In Fig. 1(B), the second path reaches a point known to be in Bader region 1 after just two ascent steps, allowing the path to be terminated early. Each point along the ascent path from (i_2,j_2,k_2) is then assigned to the region corresponding to m_1. When an ascent path from a point (i_n,j_n,k_n) reaches a new maximum m_2, as shown in Fig. 1(C), a new entry is made in the list of known charge density maxima and the points along the ascent path are given the value 2. When a steepest ascent trajectory has been initiated from all grid points, the partitioning analysis is complete, and all grid points have then been assigned to a Bader region. This assignment of the grid points to Bader regions is all that is needed for further analysis such as calculations of partial charges or multipole

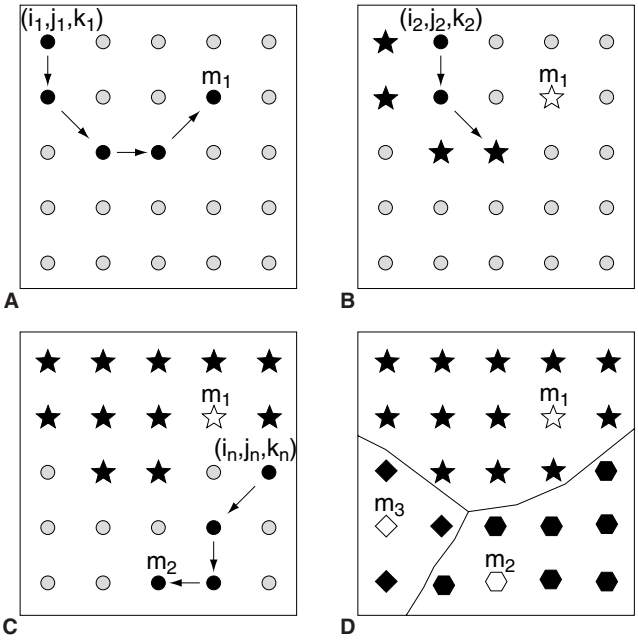

Fig. 1. An illustration of the steepest ascent paths on the charge density grid that are used to find Bader regions. (A) The first path starts from point (i_1,j_1,k_1) and after four steepest ascent moves ends at point m_1, a point of maximum charge density. Each point along the path is assigned to the region associated with m_1. (B) The second path starts from (i_2,j_2,k_2) and is terminated after two moves when it reaches a point which has already been assigned to m_1 (stars indicate points assigned to region 1). This process is repeated from each unassigned grid point. (C) Starting from the point (i_n,j_n,k_n), a new maximum m_2 is found and all grid points which lead to this maximum are assigned to m_1. (D) After all grid points have been assigned, three maxima have emerged and the three groups of grid points are shown with stars for m_1, hexagons for m_2 and diamonds for m_3.

moments. The total electronic charge of each Bader region can be found by summing over the grid points assigned to that region, and the approximate location of the dividing surfaces can be visualized by rendering the charge density of each region separately.

This grid based analysis is highly efficient. Since the steepest ascent paths get terminated when a previously assigned point has been reached, there is a fixed amount of work required for each grid point. This is dominated by the calculation of the $\nabla\rho$ derivatives, requiring only 26 subtraction and multiplication operations per grid point, and the same number of comparisons. The computational effort, therefore, scales linearly with the number of grid points and is independent of the number of atoms in the system. Typically the analysis takes a comparable amount of time as simply reading the charge density data from disk in the computer. The analysis of a 200^3 grid takes less than a minute on a computer with a 1.8 GHz Athlon processor.

2.1. Applications

We first describe results of calculations on three simple test systems where comparison can be made with other Bader analysis algorithms, (a) a water molecule, (b) NaCl crystal, and (c) MgO crystal. We then describe an application to a study of electronic activity of a cluster of boron dopant atoms in a silicon crystal.

2.1.1. Water molecule

The structure and charge density of a water molecule was calculated with the aug-cc-pVDZ basis using Gaussian 98 [17] at the MP2 level of perturbation theory. A charge density was written as a 201^3 grid in the cube file format. On a computer with a 1.8 GHz Athlon processor, the 100 MB file took 18 s to load, and 40 s to analyze. Three Bader regions were found, each containing one atom. The total charge in each one of the regions around the hydrogen atoms contained 0.4238 electrons and the oxygen region contained 9.1566 electrons, which gives a sum of 10.0041 electrons. The atomic partial charges are the same as found by Bader [2] (see Table 1), showing that these two different algorithms yield the same results.

Table 1
Partial charge of oxygen and hydrogen in an isolated water molecule

	Partial charge	
	O atom	H atoms
Bader's original work	−1.16	+0.58
This work	−1.157	+0.576

The results of the present analysis, based on a 201^3 change density generated from an MP2 calculation with the aug-cc-pVDZ basis set, agree well with the results of Bader using an algorithm based on critical point analysis [2].

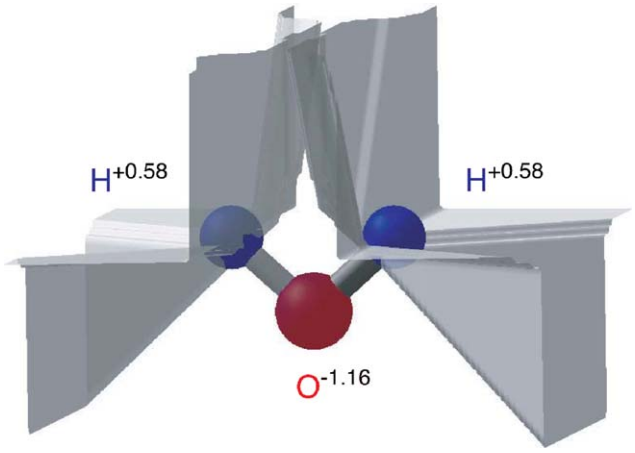

Fig. 2. Dividing surfaces separating the oxygen and hydrogen Bader regions in a water molecule. The integration over the Bader regions indicates that 0.58 e are transferred from each hydrogen atom to the oxygen atom.

The Bader surfaces for H_2O are shown in Fig. 2. It is typical of Bader surfaces to have sharp corners because the Bader volumes around atoms must tile to fill space. It is also remarkable in the case of H_2O how different the Bader volumes are from a Voronoi partitioning. Charge density in the region between the hydrogen atoms is associated with the oxygen atom, even though the hydrogen atoms are closer by.

2.1.2. NaCl crystal

As another simple test problem, we have calculated the charge on the ions in a NaCl crystal. Plane-wave based DFT calculations were performed using the VASP code [18–20] on an eight atom NaCl cell using a PAW (projector augmented wave) procedure [21,22] and the PW91 approximation to the density functional. The system contains a total of 64 electrons, nine from each of the Na atoms and seven from each of the Cl atoms. A default plane wave energy cutoff in VASP was used, 700 eV (equivalent to 51.5 Ry). The Brillouin zone was sampled with $2\times2\times2$ Monkhorst–Pack k-point mesh. A lattice constant of 5.68 Å was found to minimize the energy. The DFT calculation was repeated for various values of the density of the secondary grid used in connection with the PAW procedure. This determines the mesh size of the charge density grid obtained from the DFT calculations which is the input for the Bader analysis. Calculations were done for grids ranging from the default size of 60^3 points and up to a grid with 250^3 points. The spacing between adjacent grid points is 0.095 Å in the former case, and 0.023 Å in the latter. The CPU time in the DFT calculation is dominated by FFTs and is roughly proportional to the number of grid points. However, a calculation with a finer grid only needs to be done once after the optimized atomic coordinates have been found. Furthermore, the output from

a calculation with a courser grid can be used as input for a calculation on a finer grid in many codes, for example VASP. For NaCl, only six electronic iterations were needed to converge a calculation with a 100^3 grid when the result of a calculation with a 60^3 grid was used as input, while a calculation starting with no information about the wave function requires 15 electronic iterations. In calculations based on pseudopotentials or PAW, such as this one, it is often advisable in any case to carry out a separate DFT calculation for the charge density analysis so as to include more electrons explicitly (i.e. fewer electrons represented by the pseudo-potential or frozen core) than during the optimization of the atomic coordinates.

One indication of the quality of the result of the Bader analysis is the total number of electrons obtained from the integration over all the Bader regions (i.e. the conservation of charge). When using the 60^3 grid, the total number of electrons is reproduced with an error less than 10^{-4}. The error drops to 10^{-6} when using a grid with 160^3 points. The variation in the magnitude of the charge on the eight ions in the system is 0.03 e in the former case and 0.01 e in the latter. The charge on the Na^+ ions was found to be 0.863 e when using the default grid, 0.871 e with a 100^3 grid and 0.866 e with a 250^3 grid. Convergence in the atomic charge with respect to the plane wave energy cutoff was reached at 700 eV. For most practical purposes, a 0.01 e error in the atomic charge is not of concern, especially given the inherent arbitrariness in the definition of an atomic charge in an extended system (such as a molecule or a solid). The method is, therefore, found to be sufficiently accurate for most purposes in this case by using just the default grid size, even though no interpolation between the grid points is carried out. Using the default 60^3 grid, the Bader analysis took 0.8 s of CPU time on a 1.8 GHz Athlon based computer. Simply reading the charge density file took nearly as long, 0.6 s.

Katan et al. [13] also carried out Bader analysis of NaCl from a density grid obtained by DFT using the PAW representation of core electrons. Their method is based on three-dimensional cubic spline interpolation between the grid points and a Newton–Raphson procedure to locate critical points and dividing surfaces, followed by integration along radial directions away from nuclear positions. From calculations using a rather fine electron density grid, with a mesh size of 0.050 Å, they report a charge of 0.8282 e for the Na-ions and a charge of −0.8648 e for the Cl-ions. The difference in the magnitude of the charge of the anion and cation presumably indicates errors in the numerical integration over the Bader regions. When they used a very fine grid with a mesh size of 0.033 Å, the difference in the magnitude of the charges was reduced to 0.01 e. This comparison shows, surprisingly, that their algorithm requires just as fine a grid as our algorithm to converge the atomic charges to within 0.01 e, even though it involves interpolation between the grid points and is computationally more demanding.

2.1.3. MgO crystal

We finally describe briefly calculations of atomic charges in MgO. An analysis of the Madelung field outside a MgO slab calculated using DFT with the LDA functional has given an estimate of 1.8 e [23]. An application of the AIMPAC algorithm of Bader [2] as implemented in the ABINIT software [24] on a charge density grid generated from DFT calculations gave the value 1.72 e [25]. Our method applied to a similar charge density grid gives the same value, 1.72 e [26]. This illustrates further that our algorithm gives similar results to the original algorithm of Bader and that the charges obtained are in good agreement with the modeling of the electrical field.

2.1.4. Activity of B-clusters

We now describe briefly the results of Bader analysis of a three-atom boron cluster within a silicon crystal. Boron is used in semiconductor technology to p-dope silicon, making it conductive by hole transport. As devices are made smaller, the concentration of dopant atoms needs to be increased. In current devices, the concentration of boron atoms is at or past the thermodynamic solubility limit and boron clusters tend to form. Cluster formation is known to reduce the electrical activity of the dopant atoms. A particularly stable cluster is the B_3I^- cluster [27] shown in Fig. 3. The B_3 indicates that this cluster has three boron atoms, and the I refers to the fact that the total number of atoms is one greater than in the perfect silicon crystal. In order to model diffusion and electrical activity of dopant atoms, it is important to have information about the stability and electrical activity of such clusters. Short time annealing at high temperature is used to break the clusters up to a large extent in today's technology. Experimental measurements have shown that annealing at about 1000 °C for a few seconds brings the electrical activity to on the order of 50% of what would be expected from fully dispersed boron dopant atoms [28]. At that stage, the order in the Si crystal is presumably largely restored and large B-clusters broken up, but some particularly stable B-clusters remain. Nearly full electronic activity is obtained after ca. 100 s.

Density functional theory calculations were carried out for the a linear configuration of the B_3I cluster in a silicon crystal (see Fig. 3). This has been shown to be a particularly stable boron cluster and is likely to survive short time annealing [27]. The PW91 functional was used with plane wave basis set up to a 231 eV cutoff and ultrasoft pseudopotentials [29]. The calculations were carried out using the VASP code [18–20]. A $2\times2\times2$ Monkhorst–Pack k-point mesh was found to give a

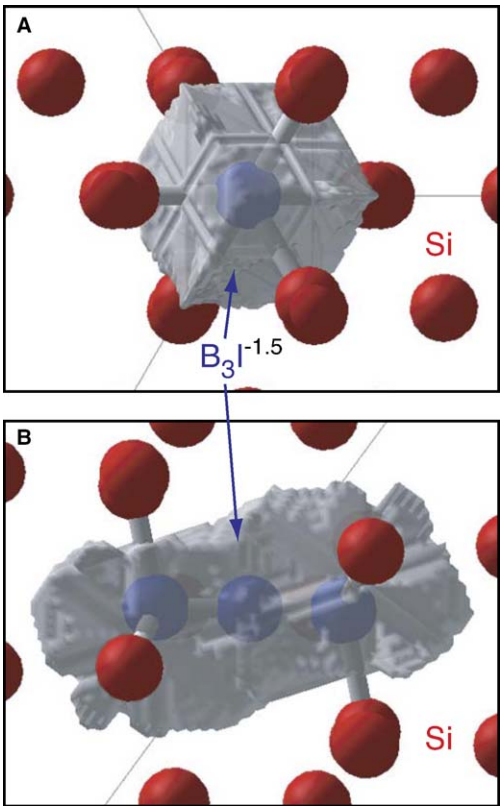

Fig. 3. End-on view (A) and side-view (B) of the Bader surface around three atom boron cluster in a silicon crystal. Integration over the Bader region indicates that 1.5 e have been transferred from the silicon atoms to the boron cluster, suggesting that the cluster has about 50% of the electronic activity of three substitutional B atoms.

sufficient sampling of the Brillouin zone. The simulation cell contains a total of 62 silicon atoms and three boron atoms. An extra electron was added to the unit cell because it is thought that the lowest energy structure of B_3I is negatively charged [27].

The charge density was generated on a grid with 88^3 points. The resulting 12 MB file was read in 2 s and analyzed in 3 s on the 1.8 GHz Athlon computer. The dividing surface around the Bader regions corresponding to the boron cluster is shown in Fig. 3. The total charge contained within these regions is 10.5 e. Each boron has a valance charge of three electrons, so the overall predicted charge of the cluster is −1.5 e. A single substitutional boron atom in a silicon crystal is found to have a charge of −0.9 e, so the Bader analysis suggests that formation of B_3I clusters reduces boron electronic activity by ca. 50%. Previous analysis of the activity of dopant clusters has been based on estimates of the relative stability of systems with different number of electrons. Such calculations of neutral, −1 and −2 charged B_3I in silicon systems have indicated that the −1 charge is the most stable state [27], which is quite consistent with our results. The Bader analysis presented here may be a more direct and a much faster way to determine the electronic activity by directly estimating the charge on the boron cluster. Further analysis of the electrical activity of boron and other dopant clusters in silicon will be presented elsewhere.

3. Scaling of effort

A major advantage of the algorithm presented here over other algorithms for Bader analysis we are aware of is its speed. Other algorithms are based on finding the location of critical points and representing the dividing surfaces for the electron density, both of which are very challenging tasks. These are particularly important considerations in solid state systems where a calculation may include on the order of 10^2 atoms as in the boron dopant cluster problem discussed above.

The algorithm presented here can easily be applied to large systems. There is a fixed computational effort per electron density grid point and the overall computer time, therefore, scales linearly with the number of grid points. Fig. 4 shows the computer time required to analyze charge density files of various sizes for the boron cluster in silicon. Cubic grids ranging from 88^3 to 200^3 points were analyzed in times between 3 s and 45 s on the 1.8 GHz Athlon based computer. The computer time clearly scales linearly with the number of grid points. The slope of the line corresponds to analyzing a million grid points in 5.6 s. The largest charge density grid with 201^3 points was generated from a calculation of a H_2O molecule. This three atom system required the same computational effort as the 65 atom boron cluster system with a similar grid size, showing that the computer time neither depends upon the number of atoms in the system nor the bonding topology.

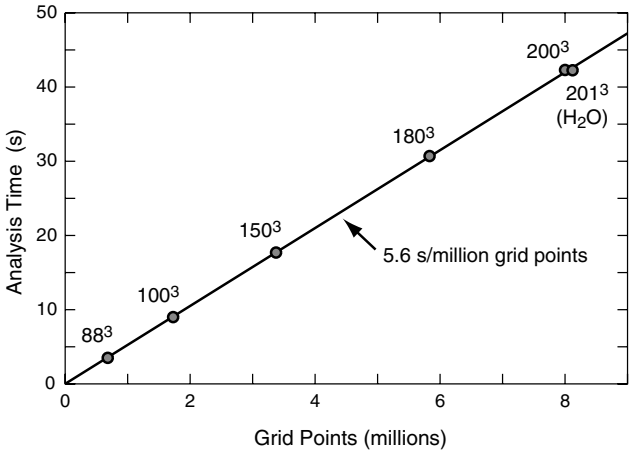

Fig. 4. Timing results for the Bader analysis of a triatomic boron cluster in silicon. The computer time scales linearly with the number of grid points in the charge density file. A charge density file generated from H_2O (the last point) takes the same amount of time to analyze as the 65 atom B_3I cluster, showing that the computer time is independent of the number of atoms in the system.

The software including source code for the Bader analysis program described here, as well as instructions for running the program are available on the web site http://theory.cm.utexas.edu/bader.

4. Summary

We have presented here a simple and yet efficient algorithm for dividing up electron density of molecules and condensed phase systems using the partitioning criteria proposed by Bader. The method is fast and robust while the computational effort scales linearly with the number of grid points. The time it takes to carry out the analysis is on the order of the time it takes to read in the electron density grid data from the computer's hard disk. The method was tested by assigning charges to atoms in a water molecule and in a NaCl crystal. Our results agree well with results obtained with other Bader analysis algorithms. We have, furthermore, used the method to analyze electrical activity of a three-atom boron cluster in a silicon crystal, B_3I. The cluster was found to have a charge of -1.5 e which indicates half as large electrical activity as compared with three substitutional boron atoms.

Acknowledgements

We would like to thank Fernando Vila for generating the Gaussian charge densities cube files for a water molecule and Hugo Bohorquez for helpful suggestions regarding the manuscript. This work was funded by NSF under grant CHE-0111468 and by LSI Logic Inc. through a grant from the Semiconductor Research Corporation. GH acknowledges support from the Robert A. Welch Foundation under grant no. F-1601.

References

[1] F.D. Proft, C.V. Alsenoy, A. Peeters, W. Langenaeker, P. Geerlings, J. Comput. Chem. 23 (2002) 1198.
[2] R. Bader, Atoms in Molecules: A Quantum Theory, Oxford University Press, New York, 1990.
[3] P.L.A. Popelier, Theor. Chem. Acc. 105 (2001) 393.
[4] P.L.A. Popelier, MORPHY98, A program written by P.L.A. Popelier with a contribution from R.G.A. Bone. UMIST, Manchester, England, 1998.
[5] B.B. Stefanov, J. Cioslowski, J. Comput. Chem. 16 (1995) 1394.
[6] P.L.A. Popelier, Theor. Chim. Acta 87 (1994) 465.
[7] P.L.A. Popelier, Comp. Phys. Commun. 108 (1998) 180.
[8] N.O.J. Malcolm, P.L.A. Popelier, J. Comput. Chem. 24 (2003) 437.
[9] N.O.J. Malcolm, P.L.A. Popelier, J. Comput. Chem. 24 (2003) 1276.
[10] S. Noury, X. Krokidis, F. Fuster, B. Silvi, Comput. Chem. 23 (1997) 597.
[11] B. Silvi, C. Gatti, J. Phys. Chem. A 104 (2000) 947.
[12] B.P. Uberuaga, E.R. Batista, H. Jónsson, J. Chem. Phys. 111 (1999) 10664.
[13] C. Katan, P. Rabiller, C. Lecomte, M. Guezo, V. Oison, M. Souhassou, J. Appl. Cryst. 36 (2003) 65.
[14] Y. Aray, J. Rodríguez, J. Rivero, J. Phys. Chem. A 101 (1997) 6976.
[15] G.K.H. Madsen, C. Gatti, B.B. Iversen, L. Damjavonic, G.D. Stucky, V.I. Srdanov, Phys. Rev. B 59 (1999) 12359.
[16] F.W.B. König, R.F.W. Bader, T. Tang, J. Comput. Chem. 3 (1998) 317.
[17] M.J. Frisch, G.W. Trucks, H.B. Schlegel, M.A.R.G.E. Scuseria, J.R. Cheeseman, V.G. Zakrzewski, J.J.A. Montgomery, R.E. Stratmann, J.C. Burant, S. Dapprich, J.M. Millam, A.D. Daniels, K.N. Kudin, M.C. Strain, O. Farkas, J. Tomasi, V. Barone, M. Cossi, R. Cammi, B. Mennucci, C. Pomelli, C. Adamo, S. Clifford, J. Ochterski, G.A. Petersson, P.Y. Ayala, Q. Cui, K. Morokuma, D.K. Malick, A.D. Rabuck, K. Raghavachari, J.B. Foresman, J. Cioslowski, J.V. Ortiz, A.G. Baboul, B.B. Stefanov, G. Liu, A. Liashenko, P. Piskorz, I. Komaromi, R. Gomperts, R.L. Martin, D.J. Fox, T. Keith, M.A. Al-Laham, C.Y. Peng, A. Nanayakkara, C. Gonzalez, M. Challacombe, P.M.W. Gill, B. Johnson, W. Chen, M.W. Wong, J.L. Andres, C. Gonzalez, M. Head-Gordon, E.S. Replogle, J.A. Pople, Gaussian 98, Revision A. 7, Gaussian Inc., Pittsburgh PA, 1998.
[18] G. Kresse, J. Hafner, Phys. Rev. B 47 (1993) 558.
[19] G. Kresse, J. Hafner, Phys. Rev. B 49 (1994) 14251.
[20] G. Kresse, J. Furthmüller, Comput. Mater. Sci. 6 (1996) 16.
[21] P.E. Blöchl, Phys. Rev. B 50 (1994) 17953.
[22] G. Kresse, J. Joubert, Phys. Rev. B 59 (1999) 1758.
[23] U. Berkenheuer, N. Rösch, J.C. Boettger, J. Chem. Phys. 100 (1994) 6826.
[24] X. Gonze, J.M. Beuken, R. Caracas, F. Detraux, M. Fuchs, G.-M. Rignanese, L. Sindic, M. Verstraete, G. Zerah, F. Jollet, M. Torrent, A. Roy, M. Mikami, P. Ghosez, J.-Y. Raty, D. Allan, Comput. Mater. Sci. 25 (2002) 478.
[25] C. Noguera, A. Pojani, P. Casek, F. Finocchi, Surf. Sci. 507–510 (2002) 245.
[26] B.P. Uberuaga, R. Smith, A.R. Cleave, G. Henkelman, R.W. Grimes, A.F. Voter, K.E. Sickafus, Phys. Rev. B 71 (2005) 104102.
[27] X.-Y. Liu, W. Windl, M.P. Masquelier, Appl. Phys. Lett. 77 (2000) 2018.
[28] M. Aboy, L. Pelaz, L.A. Marqués, J. Barbolla, A. Mokhberi, Y. Takamura, P.B. Griffin, J.D. Plummer, Appl. Phys. Lett. 83 (2003) 4166.
[29] D. Vanderbilt, Phys. Rev. B 41 (1990) 7892.